Transcriptional profile of postmortem skeletal muscle

Despina Sanoudou, Peter B. Kang, Judith N. Haslett, Mei Han, Louis M. Kunkel and Alan H. Beggs

Physiol Genomics 16:222-228, 2004. First published Nov 18, 2003;
doi:10.1152/physiolgenomics.00137.2003

Physiological Genomics publishes results of a wide variety of studies from human and from informative model systems with techniques linking genes and pathways to physiology, from prokaryotes to eukaryotes. It is published quarterly in January, April, July, and October by the American Physiological Society, 9650 Rockville Pike, Bethesda MD 20814-3991. ISSN: 1094-8341, ESSN: 1531-2267. Visit our website at http://www.the-aps.org/.

Physiol Genomics 16: 222–228, 2004.
First published November 18, 2003; 10.1152/physiolgenomics.00137.2003.

Transcriptional profile of postmortem skeletal muscle

Despina Sanoudou,[1,3] Peter B. Kang,[1,2,3] Judith N. Haslett,[1,3] Mei Han,[1,3] Louis M. Kunkel,[1,3] and Alan H. Beggs[1,3]

[1]*Genetics Division and Genomics Program,* [2]*Neurology Department, Children's Hospital; and* [3]*Harvard Medical School, Boston, Massachusetts 02115*

Submitted 20 August 2003; accepted in final form 4 November 2003

Sanoudou, Despina, Peter B. Kang, Judith N. Haslett, Mei Han, Louis M. Kunkel, and Alan H. Beggs. Transcriptional profile of postmortem skeletal muscle. *Physiol Genomics* 16: 222–228, 2004. First published November 18, 2003; 10.1152/physiolgenomics.00137.2003.—Autopsy specimens are often used in molecular biological studies of disease pathophysiology. However, few analyses have focused specifically on postmortem changes in skeletal muscles, and almost all of those investigate protein or metabolic changes. Although some structural and enzymatic changes have been described, the sequence of transcriptional events associated with these remains unclear. We analyzed a series of new and preexisting human skeletal muscle data sets on ≃12,500 genes and expressed sequence tags (ESTs) generated by the Affymetrix U95Av2 GeneChips from seven autopsy and seven surgical specimens. Remarkably, postmortem specimens (up to 46 h) revealed a significant and prominent upregulation of transcripts involved with protein biosynthesis. Additional upregulated transcripts are associated with cellular responses to oxidative stress, hypoxia, and ischemia; however, only a subset of genes in these pathways was affected. Overexpression was also seen for apoptosis-related, cell cycle regulation/arrest-related, and signal transduction-related genes. No major gene expression differences were seen between autopsy specimens with <20-h and 34- to 46-h postmortem intervals or between pediatric and adult cases. These data demonstrate that, likely in response to hypoxia and oxidative stress, skeletal muscle undergoes a highly active transcriptional, and possibly, translational phase during the initial 46-h postmortem interval. Knowledge of these changes is important for proper interpretation of gene expression studies utilizing autopsy specimens.

autopsy; surgical; microarrays; gene expression

CELLULAR CHANGES OCCURRING in postmortem muscle have been the subject of several studies, as they have a significant impact in clinical research and forensic science. Structural, metabolic, and other protein changes have been investigated using primarily electron microscopy, histochemistry, and sodium dodecyl sulfate-polyacrylamide gel electrophoresis (SDS-PAGE) in a range of different species, and to a lesser extent, in human skeletal and cardiac muscle (2, 4, 11, 38). Some key postmortem changes include the accumulation of toxins, ischemia or anoxia, alteration of pH, membrane damage with diffusion, disruption of homeostasis, and eventually cessation of cellular biosynthetic activity. More specifically, anoxia leads to accumulation of lactic acid, which in turn decreases the tissue pH with increasing postmortem interval. The cellular pH is important in determining the level of activity of specific subsets of proteases and consequently the level of protein degradation (28). The integrity of the plasma membrane has also been shown to be compromised after death, thus allowing the diffusion of ions in and out of the cell (39). The increase of intracellular ion levels, and especially of Ca^{2+}, stimulates a series of molecular events such as the activation of calmodulin, calmodulin binding proteins, and Ca^{2+}-dependent proteases, (e.g., calpain) (24, 45). Histochemical studies of postmortem muscle have detected the rapid disappearance of glycogen and phosphorylase, the increase of glucose and lactate concentrations, and varying levels of enzymatic deficits including, for example, isocitric dehydrogenase, cytochrome oxidase, and β-hydroxybutyrate dehydrogenase (2, 4).

In animal models it has been shown that the postmortem interval, the storage temperature, and the administration of protease inhibitors shortly before death have a significant impact on postmortem modifications in muscle (38). Overall, electron microscopy of rat skeletal muscle at a storage temperature of around 20°C and without protease inhibitor treatment revealed the following: swollen mitochondria by 2 h postmortem; loss of ribosomes and glycogen, rupture of the I bands, and appearance of small membranous bodies by 12 h; and collapse of the I bands, loss of Z lines and appearance of large membranous bodies by 24–48 h (11). At the same temperature, rat skeletal muscle myofibrillar protease activity increased linearly with postmortem time of storage, whereas creatine phosphokinase activity decreased linearly with time (27). Glycogen has been shown to degrade rapidly after death, whereas glucose and lactate concentrations increase (4). At the transcriptional level a small number of individual genes have been studied in autopsy of heart and/or skeletal muscle, predominantly in the context of heart disease (17, 35, 47). However, the sequence of transcriptional events that occur postmortem remains unclear.

Several microarray-based studies of gene expression in normal and diseased states have been performed on human skeletal muscles obtained at biopsy or autopsy (1, 8, 20, 21, 33) and on murine skeletal muscle obtained immediately postmortem (30, 32, 37, 40). These studies identified a number of genes in various functional categories that are differentially expressed in the disease states, suggesting that major alterations in tissue have far-reaching consequences for gene expression. Skeletal muscle tissue obtained at autopsy would be expected to have similarly extensive changes compared with tissue obtained at biopsy. However, no gene expression studies addressing this particular issue have been published to date, either in humans or mice.

We studied seven autopsy and seven surgical human skeletal muscle specimens using oligonucleotide Affymetrix GeneChip arrays (U95Av2) that contain representative sequences from over 12,000 known genes and expressed sequence tags (ESTs). The data sets from 12 of these 14 samples have been previously published as part of the normal control baseline in a study on

Article published online before print. See web site for date of publication (http://physiolgenomics.physiology.org).

Address for reprint requests and other correspondence: A. H. Beggs, Genetics Division, Children's Hospital Boston, 300 Longwood Ave., Boston, MA 02115 (E-mail: beggs@enders.tch.harvard.edu).

nemaline myopathy (33). In that study, significant disease-related gene expression changes were identified, particularly in the glycolytic energy metabolism pathway (decreased), in connective tissue-related genes (increased), and in muscle satellite cells (increased). The aim of the current study was to understand gene expression changes that occur in normal human muscle postmortem and to relate these to histological reports and previous studies at the protein and metabolic levels. Remarkably, our findings provide evidence for a very active transcriptional phase in skeletal muscle during the first 46 h postmortem. Although these tissues are clearly subject to ischemia and hypoxia, genes for only some components of the ischemia and hypoxia-response pathways are transcriptionally upregulated under these conditions. These data provide an important baseline for future studies of diseased muscle obtained surgically and at various portmortem intervals.

MATERIALS AND METHODS

Human samples and microarray experiments. Affymetrix GeneChip data sets from 12 snap-frozen skeletal muscle specimens, from individuals unaffected by muscle disease (surgical specimens *T142*, *T146*, *T147*, *T172*, *T180*, and *T181*; autopsy specimens *T149*, *T160*, *T170*, *T177*, *T178*, *T179*) were generated as previously described (33). Two additional skeletal muscle specimens were prepared specifically for this study (*T256*, surgical specimen from a 38-yr-old female; and *T289*, autopsy specimen from a 1-yr-old male). The postmortem interval of the autopsy specimens ranged between 16 and 46 h (Table 1). Tissue was most commonly obtained from the quadriceps, but other muscles are also represented (Table 1). An effort was made to match the ages of the individuals whose specimens were used. Three surgical and three autopsy specimens were from children younger than 4 yr, whereas four surgical and four autopsy specimens were from adults older than 37 yr. All samples were obtained under institutionally approved human subjects protocols.

RNA extraction (6–8 μg from each tissue sample), target preparation, and hybridization to Affymetrix U95Av2 GeneChips, were performed as previously described (33). The U95Av2 GeneChip contains 12,626 annotated genes and ESTs. The data are available at the Gene Expression Omnibus (GEO) web site under the series number GSE595 (**http://www.ncbi.nlm.nih.gov/geo/**).

Data analysis. The data sets originating from the 14 specimens were first processed by the Affymetrix MicroArray Suite 5.0 software (MAS5.0), and signal values (reflecting expression levels) and "present/absent" calls (an Affymetrix computed measure representing confidence in gene expression presence) were computed for each probe set. The signal values were not normalized at this stage, although signal values were adjusted to an overall target intensity of 1,500. The correlation coefficients (r) were calculated for all 14 data set pair wise comparisons.

For hierarchical clustering, we used average linkage as previously described, with centered linear correlation as a measure of similarity (19). This approach clusters both specimens and probe sets on two different axes. The selected filters removed probe sets with an "absent" call across all 14 samples or a standard deviation (SD) $\leq$1,000. The SD filter is applied to facilitate the clustering of samples, by removing probe sets with very similar expression across all samples that are therefore likely to act as noise in the specific type of analysis. The resulting 2,116 probe sets were processed using the Cluster and TreeView Software (18).

A permutation analysis was performed to evaluate the robustness of the sample clustering. Hierarchical clustering was run seven additional times, each time removing one randomly chosen data set from each of the two main clusters that were originally identified (autopsy and surgical). Thus two different data sets were removed for each of the seven permutations.

Significance analysis of microarrays (SAM) was used to identify significant fold changes between autopsy and surgical specimens as described (41). Prior to this analysis all data sets were normalized to a slope of 1 with a reference data set. The reference data set was created by taking the average expression of each probe set between the two data sets (one autopsy and one surgical) with the highest average correlation coefficient to all other data sets in their group (i.e., within the autopsy or surgical sample group, respectively). A two-class unpaired data analysis was performed using a Δ threshold of 1.72 [the "Δ" parameter as described by Tusher et al. (41), enables the user to examine the effect of the false-positive rate in determining significance] and a fold threshold of 2 [where "fold" is calculated as (average expression in autopsy specimens)/(average expression in surgical specimens)]. Probe sets were considered significantly changed in autopsy compared with surgical samples if they were selected at false discovery rate (FDR) cutoff of $\leq$1.66%.

The SAM analysis was repeated using only quadriceps-derived specimens ($n = 9$), to control for muscle type-dependent changes. The list of significantly changed genes in autopsy vs. surgical quadriceps samples was highly similar to the list obtained for all 14 specimens, with the same functional categories showing significant change ($\leq$3% size variation between them) and ~50% overlap between individual probe sets. The high correlation seen between specimens of different muscle types by hierarchical clustering (Fig. 1) and correlation coefficient analysis ($r = 0.84$–0.98), together with the high similarity in the significantly changed molecular pathways in all 14 specimens compared with the 9 quadriceps samples, suggest that the muscle types studied are directly comparable. Therefore, for the purpose of this study all 14 specimens were considered together.

Correlation coefficient analysis was used to identify probe sets with high r values and therefore similar expression patterns across all 14 data sets. This analysis was applied to the un-normalized signal values of all probe sets with unknown molecular functions that were significantly changed between autopsy and surgical specimens. The correlation coefficients against all 12,626 probe sets on U95Av2 GeneChips were calculated, and a cutoff of $\geq$0.900 was applied to select for highly correlated probe sets.

Supplementary Tables S1 and S2, containing complete results of the SAM and the correlation coefficient analyses, are available online at the *Physiological Genomics* web site[1] and at **http://www.chb-genomics.org/beggslab/**.

Table 1. *Clinical and histopathological information*

Surgical/Autopsy	Tissue Sample No.	Age/Sex	Muscle Type	Postmortem interval
Surgical	*T146*	1yr/M	quadriceps	
Surgical	*T142*	2yr/F	quadriceps	
Surgical	*T147*	4yr/F	quadriceps	
Surgical	*T181*	37yr/F	quadriceps	
Surgical	*T256*	38yr/F	biceps	
Surgical	*T180*	58yr/M	biceps	
Surgical	*T172*	60yr/M	quadriceps	
Autopsy	*T149*	0.08yr/M	quadriceps	18h
Autopsy	*T160*	2.8yr/M	quadriceps	43h
Autopsy	*T289*	1yr/M	quadriceps	46h
Autopsy	*T178*	55yr/F	skeletal	16h
Autopsy	*T170*	65yr/M	quadriceps	<45h
Autopsy	*T177*	67yr/M	pectoral	34h
Autopsy	*T179*	72yr/M	skeletal	20h

M, male; F, female.

[1]The Supplementary Material for this article (Tables S1 and S2) is available online at **http://physiolgenomics.physiology.org/cgi/content/full/00137.2003/DC1**.

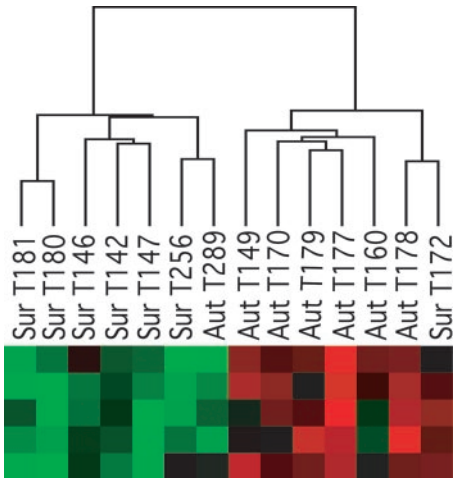

Fig. 1. Hierarchical clustering of seven autopsy and seven surgical skeletal muscle samples. The dendrogram generated by TreeView (at *top*) is indicative of the correlations between data sets for the 14 surgical (Sur) and autopsy (Aut) specimens (*middle*). *Bottom*: signal strengths for a representative gene cluster, in which each row reflects the expression levels (red = high expression, green = low expression) of one probe set across all samples.

RESULTS

Quality controls were applied to ensure that the RNA from both surgical and autopsy specimens was equally intact. These steps included visual evaluation of the total RNA sizes by agarose gel electrophoresis and assessment of the cRNA amount hybridized to the GeneChips by comparison of the measurements obtained for probe sets representative of 5′ and 3′ ends of control genes. All samples had an A260/280 absorbance ratio between 1.9 and 2.1 as measured on the spectrophotometer. The band intensity ratio for 28S to 18S rRNA was close to 2 as seen on the agarose gels, and signal ratios below 2 for 3′ vs. 5′ probe sets for β-actin and glyceraldehyde-3-phosphate dehydrogenase genes (well within the Affymetrix recommendations) as seen after hybridization to the GeneChips. In brief, skeletal muscle samples up to 46 h postmortem yielded intact, high-quality RNA.

Hierarchical clustering identified two major sample clusters: one consisting predominantly of surgical and one of autopsy samples. However, some overlap was evident between the two sample types, as one member of each group clustered with the other groups (Fig. 1). This overlap was reproducible and seen in all seven dendrograms generated during the permutation analysis. The postmortem interval of the autopsy samples did not appear to have an impact on their correlation coefficients. Hierarchical clustering demonstrated that age, muscle type (see MATERIALS AND METHODS), and postmortem interval did not appear to have a major role, and therefore surgical and autopsy samples of all ages and types were considered together for the purpose of further analysis. It is of particular interest that autopsy specimens ranging from 16 to 46 h postmortem had such similar expression patterns, suggesting that further major transcriptional changes do not occur during the postmortem interval from 16 to 46 h. An independent calculation of the correlation coefficients showed a similar range of r values within each group (r = 0.83–0.98 for surgical and r = 0.86–0.96 for autopsy) and slightly lower across groups (r = 0.76–0.96), comparable to previous analyses of patient and control specimens (33).

The SAM program was used on the 14 normalized data sets to identify significant transcriptional differences between surgical and autopsy specimens. We identified 140 probe sets as significantly overexpressed (FDR ≤ 1.66%) in autopsy vs. surgical samples (Supplementary Table S1). None of the downregulated probe sets were considered significantly changed at this FDR cutoff. The fold change of the upregulated probe sets ranged between the selected lower cutoff of 2-fold [seen for the genes tubulin-specific chaperone E (*TBCE*); eukaryotic translation initiation factor 3, subunit 6 (*EIF3S6*); and *S*-adenosylmethionine decarboxylase 1 (*AMD1*)] and 27.33-fold [seen for the gene v-maf musculoaponeurotic fibrosarcoma oncogene homolog F (*MAFF*)]. The 140 upregulated probe sets were assigned to functional categories according to their Gene Ontology (GO) annotations. The four main categories included cell death (n = 11), metabolism (n = 35), cell maintenance (n = 46), and cell communication (n = 21) (Fig. 2). Because of the large size of certain subgroups within the four categories, some of these are presented as independent categories. In total seven functional categories were created: metabolism (n = 35 probe sets), transcription (n = 26), cell cycle (n = 23), cell communication (n = 13), apoptosis (n = 11), other (n = 22), and unknown (n = 15) (Supplementary Table S1). Of the seven functional categories, some had major distinct subgroups, which are represented in Fig. 2. Genes with more than one molecular function were placed under all relevant functional categories. The metabolism-related genes were predominantly involved in protein metabolism such as biosynthesis (n = 9), protein targeting/modification (n = 7) and proteolysis (n = 5), amine metabolism (n = 4), and nucleic acid metabolism (n = 4). Although GO usually classifies transcription under nucleic acid metabolism, we have created a separate group, due to their large number, to include all transcription-related probe sets. The majority of cell cycle-related genes were associated with cell cycle arrest (n = 6) and regulation (n = 7), and a small number were M- or S-phase related (n = 2 and 5, respectively). The cell cycle category had the highest average fold change (4-fold) compared with all

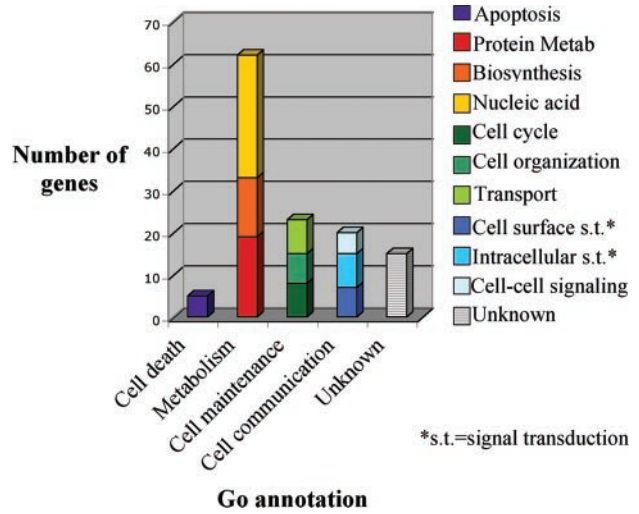

Fig. 2. The main functional categories showing significant overexpression in autopsy specimens as determined by significance analysis of microarrays (SAM). Functional categorization of the genes was based on the Gene Ontology (GO) annotations.

other categories, with cell cycle regulation and arrest showing the highest fold changes in their category. Several cytoskeleton-related ($n = 8$) and metal ion binding probe sets ($n = 5$) were also significantly upregulated, but because of the small size of these groups they were classified under "Other".

The 125 known genes showing significant overexpression were further analyzed with Osprey (3) to identify possible networks of interaction with other genes. Osprey generates gene interaction networks based on information retrieved by the General Repository for Interaction Data sets (the GRID, **http://biodata.mshri.on.ca/grid**), which in turn compiles gene annotations provided by the *Saccharomyces* Genome Database (**http://www.yeastgenome.org/**). Four interaction networks with three or more interactions with known genes were identified through this analysis (Fig. 3). They were associated with the following significantly changed genes: CCAAT-box-binding transcription factor (*CBF2*), similar to *S. cerevisiae* Sec6p and *Rattus norvegicus* rsec6 (*SEC6*), sin3-associated polypeptide 30 kDa (*SAP30*), and RAD51 homolog (RecA homolog, *Escherichia coli*) (*S. cerevisiae*) (*RAD51*). Each network contained between 5 and 24 known genes. Based on GO annotations, all of these genes are involved in cell growth and maintenance, and the majority also has a metabolic role (Fig. 3). More specifically, all *CBF2* interacting genes were cell cycle related, all *SEC6* interacting genes were metabolism related, with 4/6 genes also involved in protein transport, and 6/7 *SAP30* interacting genes were metabolism and/or transcription related. The *RAD51* network consisted of at least 24 known genes, of which 20 were metabolism related (nucleic acid metabolism = 9 genes and protein degradation = 3), and 6 were transport related. The majority of these interactions have been identified by affinity precipitation, a few of them by synthetic lethality, and five of them by the yeast two-hybrid experimental system. Of the 38 genes identified by Osprey, only 5 had representative probe sets on the U95Av2 GeneChips, and none of them was significantly changed or highly correlated, at the transcriptional level, with the 4 central genes in these networks (r range -0.62 to $+0.58$). The fold changes for the five genes ranged between -1.61 (*RAD52*) and $+4.00$ (*CPA2*), with *RAD52* and *CPA2* being the only two genes exceeding the $\geq$1.5-fold cutoff.

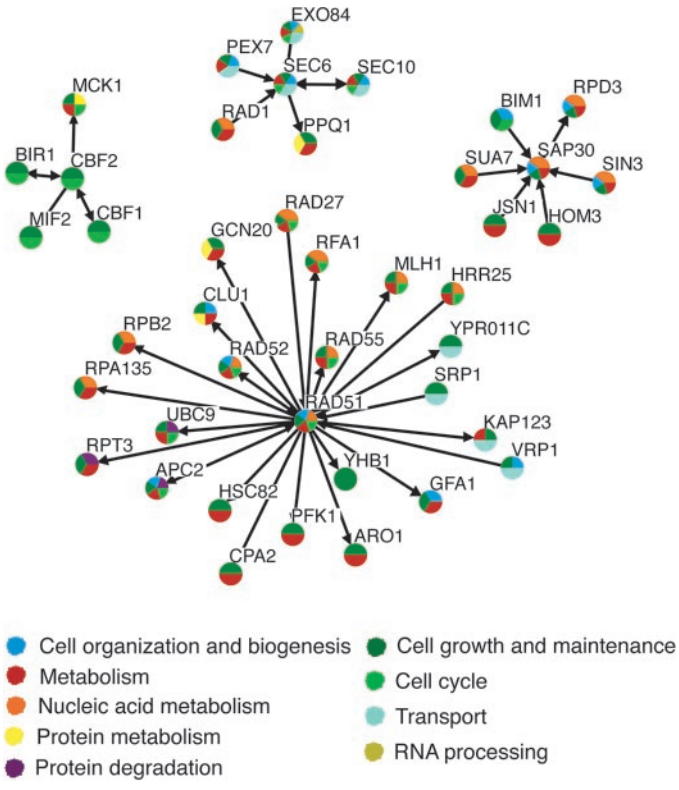

Fig. 3. Interaction networks of four significantly changed genes as identified by Osprey. Each gene known to interact with the four upregulated genes (appearing in the core of each network) is indicated by an arrow and is functionally categorized based on the GO annotations. The direction of the arrows indicates which protein has been shown to bind another.

The 15 significantly upregulated probe sets of unknown molecular function were further studied by correlation coefficient analysis against all 12,626 probe sets. Twelve of the probe sets correlated to one or more probe sets by $r \geq 0.900$ (Supplementary Table S2). When the top 50 correlations for each of the unknown probe sets were considered, a large number of them coincided with the 125 known genes identified above. The number of correlations to known genes per unknown probe set ranged between 30/50 (38683_s_at) and 7/50 (34739_at and 32835_at) (Supplementary Table S2).

DISCUSSION

Human skeletal muscle specimens obtained at autopsy are often used for diagnostic or research purposes. Previous studies have analyzed the structural and biochemical changes that occur in postmortem tissue, yet molecular alterations, including those involving gene expression, have only been examined for a handful of genes. This study is the first to describe large-scale differences in gene expression between human skeletal muscle obtained at autopsy and biopsy.

Hierarchical clustering and correlation coefficient analysis enabled us to perform a primary global analysis of the 14 data sets. These analyses classified the specimens into autopsy and biopsy dominant clusters (Fig. 1), consistent with the slightly higher intragroup ($r = 0.83$–0.98) than intergroup ($r = 0.79$–0.96) coefficient values. However, two samples, *T172* and *T289*, clustered in the "wrong" category. There were no features unique to these two samples that could account for their misclassification. *T172* represented the oldest individual in the biopsy group, but several subjects in the autopsy group were older. *T289* had the longest postmortem interval, but another sample was nearly as old. Both sample sites were quadriceps, the most common site from which muscle was obtained for this study.

Overall, the similarities within each class of specimens outweigh the similarities between classes. Although previous studies on bovine muscle have suggested that postmortem degradation of certain proteins was slower in older animals (22), age did not play a role in the clustering of our 14 specimens. A potential limitation of this study is the heterogeneity of muscle sampling sites. The scarcity of control muscle samples precluded an analysis of this size involving only one muscle type. However, the predominance of quadriceps samples and the clustering of all the nonquadriceps samples in the "correct" category (autopsy vs. biopsy) indicate that the heterogeneity of our samples did not have a significant impact on our results. Moreover, an independent analysis of quadriceps

specimens alone yielded highly similar results (data not shown).

The most prominent and unexpected change in postmortem muscle was the overall upregulation in protein synthesis. Overexpression was seen in ~26 transcription factors or transcription-related genes and an equal number of protein metabolism-related genes. The latter category included RNA binding proteins, ribosomal proteins, translation factors, amino acid/tRNA synthetases, and protein modification and targeting genes. This evidence indicates that despite expectations of an exclusively and rapid degenerative process, skeletal muscle goes through a very active transcriptional/translational phase during the first 46 h postmortem, most likely reflecting a cellular adaptive response to extracellular stimuli.

Specific transcriptional differences between the autopsy and surgical specimens were identified. The 140 probe sets with significant differences at an FDR of ≤1.66% were grouped into 7 functional categories based on GO annotations. The highest fold changes were seen in the cell cycle-related category, including genes involved in cell cycle regulation and cell cycle arrest (Supplementary Table S1). Overexpression of multiple apoptosis-related probe sets was also observed. Some examples include *GADD45A* (7.23-fold change), which participates in cell cycle arrest but also responds to environmental stress and leads to apoptosis via the p38/JNK pathway, and *NFKBIA* (2.24-fold), which can lead to apoptosis by forming a complex with p53 or inducing the activation of caspase-3 (5, 7, 36). Caspase-3 cleaves and activates the upregulated *STK3* (seen upregulated by 2.18-fold), which in turn contributes to the apoptotic response (16). Another overexpressed gene, *MYC* (3.58-, 2.3-, and 2.22-fold, for probe sets 37724_at, 1973_s_at, and 1936_s_at, respectively), has been shown to regulate the switch from cytostatic to apoptotic p53-dependent cellular response, by inhibiting p53 from activating p21 (*CIP1*) (34). Overall, autopsy skeletal muscle displays alterations in several different cell cycle and apoptosis-related pathways in response to the multiple and complex cell environment changes.

As might be expected in light of the overall process, genes involved in proteolysis appear to be upregulated in autopsy specimens (Supplementary Table S1), a finding that contrasts with observations on injured or intermittently hypoxic muscle samples (9, 46). One of the multiple roles of proteolysis is the regulation of apoptosis (25), achieved by the proteolytic activation of a range of key apoptotic pathway members (Fig. 4)(42). At least two of the apoptosis-related genes overexpressed in our analysis (*STK3*, 2.18-fold; and *GADD45A*, 7.23-fold) are known to undergo proteolytic activation (16, 26). Two additional proteolysis-associated genes (*PA2G4*, 2.08-fold; and *PSMD8*, 2.47-fold for 32584_at and 2.16-fold for 1312_at) are thought to be involved in cell cycle regulation. Furthermore, proteolysis is important for cellular homeostasis by maintaining protein concentrations at optimal levels. The upregulation of certain proteolytic pathways might therefore be expected given the apparent increase in protein biosynthesis that is suggested by the overexpression of nine related probe sets (fold change range 2.00–7.23) (Supplementary Table S1). Consistent with elevated protein synthesis, multiple protein modification-related and protein targeting-related genes were also overexpressed (fold change range 2.02–2.58). What appears to be transcriptional evidence for a potential increase in protein biosynthesis was accompanied by a widespread overexpression of transcription factors and other transcription regulatory genes. These 26 probe sets had fold changes in the range of 2.04 and 4.28. These data suggest that during the initial 46-h postmortem interval, human skeletal muscle undergoes a very active phase of increased transcription in what may be an aborted attempt to modulate translation and protein synthesis/modification/targeting in response to extrinsic (e.g., hypoxia) and intrinsic (e.g., initiation of apoptotic process) stimuli.

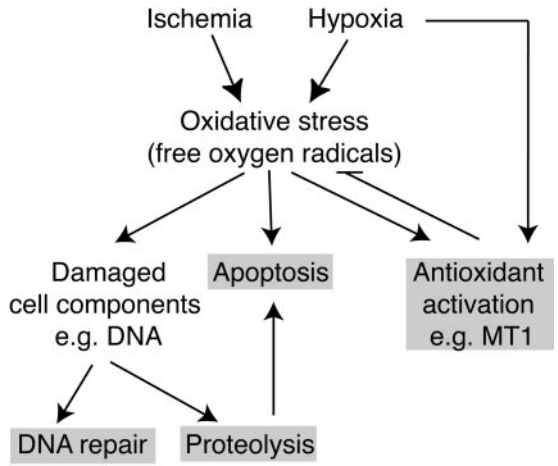

Fig. 4. Cellular pathways triggered by ischemia and hypoxia, such as seen in autopsy skeletal muscle specimens. Areas shaded gray represent processes with significant gene expression differences between surgical and autopsy specimens, as determined by SAM. MT1 = metallothionein-1.

Five metallothionein genes (*MT1A*, *MT1B*, *MT1G*, *MT1H*, *MT1L*) were upregulated by 3.34- to 4.97-fold in the postmortem specimens. Furthermore, the expression pattern of an additional upregulated (6.4-fold) probe set for an uncharacterized gene (32561_at) was highly correlated with that of the antioxidant enzyme gene, superoxide dismutase 2 (*SOD2*) (r = 0.912 by correlation coefficient analysis) (Supplementary Table S2). Metallothioneins and antioxidant enzymes play key roles in the cell, protecting against reactive oxygen species (12, 13). Hypoxia and/or ischemia, such as seen after death, have been shown to cause oxidative stress and trigger the generation of free oxygen radicals (13), as well as to transcriptionally activate metallothionein-1 genes (Fig. 4) (29). Reactive oxygen species can damage vital cell components including DNA and lead to apoptosis (6, 13). In addition to the activation of antioxidants, proteolysis is the second line of defense by systematically recognizing and removing all injured cellular components (Fig. 4)(15).

In association with this upregulation of cell cycle- and apoptotic-, proteolytic-, and antioxidant-related transcripts, two DNA repair genes (*GADD45A*, 7.23-fold; and *RAD51*, 3.90-fold) are also induced, suggesting a coordinated cellular response involving multiple pathways (Fig. 4). *RAD51* has multiple interactions at the protein level with metabolic (especially nucleic acid metabolism) and cell cycle genes, as revealed by the interaction network analysis performed based on the *Saccharomyces* Genome Database (**http://www.yeastgenome.org/**) (Fig. 3). We hypothesize that the DNA damage induced postmortem triggers the expression of DNA repair genes such as *RAD51*, which in turn stimulates a range of intracellular cascades including cell cycle regulators (14). At

least parts of these cascades are likely to be regulated at the protein level as suggested by the interaction networks and the absence of high correlation between the transcription patterns of these genes. Accordingly, 14 cell cycle regulation-, G_1/S-, S-, and G_2/M phase-related genes were overexpressed in autopsy skeletal muscle (fold range 2.04 to 27.33) (Supplementary Table S1), and multiple members of the *CBF2* and *SEC6* interaction networks have roles in the cell cycle (Fig. 3). Increased expression of cell cycle genes has also been described in relation to cardiotoxin-induced muscle injury (46). Additional gene expression changes in injured muscle have been reported for DNA replication factors, cyclins, Rb/E2f/DP, and myogenic transcription factors, as well as structural and receptor proteins (46). Five of these genes had a >1.5-fold change (*CDKN1A*, *CHRNA1*, *IFG2*, *PEG3*, *VEGF*, and *CDKN1C*), but none of them appeared significantly changed in our postmortem specimens.

Unlike previous studies on autopsy muscle specimens, no highly significant (for our thresholds) expression changes were seen for genes related to energy metabolism, muscle structure, Ca^{2+} homeostasis, or Ca^{2+}-dependent proteases such as previously described at the histochemical level (2, 4, 27, 38, 45). There were also no significant changes in stress proteins (heat shock proteins), which are usually synthesized in response to muscle injury (10). This apparent disparity may be due in part to different postmortem time points used in these studies, differences between transcript and protein level/activation, as well as the highly stringent criteria applied to selection of "significantly changed" probe sets in the present study.

Intermittent and chronic hypoxia in skeletal muscle have been shown to affect cellular processes such as the increase of type 1 myosin heavy chain, the increased activity of tricarboxylic acid cycle and the decrease of lactate dehydrogenase (9, 31). Exercise under hypoxic conditions activated the hypoxia-inducible factor 1 (*HIF1*) and seemed to influence the expression of the vascular endothelial growth factor (*VEGF*), myoglobin (*MB*), and phosphofructokinase (*PFK*) (43). No significant gene expression changes were evident for these pathways in our analysis, but *HIF1A* and *VEGF* had a >1.6-fold increase, and phosphofructokinase in yeast has been shown to interact with the RAD51 protein, which was upregulated 3.9-fold in our analysis (Fig. 3). It is still unclear whether hypoxia-inducible factor 1 activity is regulated transcriptionally or posttranscriptionally, with one recent study describing its regulation by the ubiquitin-proteasome pathway and hence supporting the latter model (23, 44). Overall, postmortem skeletal muscle shares only some of the gene expression changes seen in living tissues responding to hypoxia.

In support of the observations above, the 15 probe sets of unknown molecular function identified as significantly overexpressed in our analysis had many high correlations with the 125 known genes (Supplementary Table S2), indicating their highly similar expression patterns across all 14 muscle specimens studied. Moreover, high correlations with additional members of the major affected pathways described are seen, such as transcription, translation, nucleic acid binding, and signal transduction.

Nucleic acids extracted from autopsy specimens are often used in clinical research either because of the nature of the study or lack of suitable biopsies. The present study demonstrates that mRNA remains sufficiently intact for microarray analysis in autopsy skeletal muscle up to 46 h postmortem and that no major transcriptional differences exist between specimens of <20-h and 34- to 46-h postmortem intervals. The list of genes significantly changed between autopsy and surgical specimens is a useful resource for interpreting future studies combining the two types of skeletal muscle specimens. As an example, in our previous study on nemaline myopathy, combining autopsy and surgical specimens, only one of the 206 (0.48%) genes identified there, namely glutamine synthase (*GLUL*), overlapped with the current list, supporting that all pathways identified were disease related and not due to the surgical/autopsy nature of the specimens (33). Extra care should be taken in those studies where postmortem changes may overlap with disease processes, thus making the distinction of the two a challenging task.

During the initial 46-h postmortem interval, human skeletal muscle undergoes an active transcriptional phase. Genes for proteins involved with transcriptional and translational pathways are transcriptionally induced, potentially leading to synthesis of multiple new proteins. These data suggest activation of several pathways involving protein modification, targeting, and transport. Postmortem muscle also upregulates expression of cell protective (e.g., metallothioneins), cytostatic (e.g., cell cycle regulation- and arrest-related genes) and proteolysis-related genes. The observed overexpression of several apoptosis-related genes suggests the initiation of this process; however, the absence of other key apoptotic markers among the overexpressed genes suggests this process deviates from the physiological apoptotic process seen during life. Finally, although there is some overlap with injured and hypoxic tissue, the specific combination of gene expression changes identified in our analysis of postmortem muscle tissue appears largely to have a distinct profile.

ACKNOWLEDGMENTS

We thank to John Czerkowicz for excellent technical assistance in computer programming and Isaac S. Kohane for invaluable advice on data analysis.

GRANTS

Microarray experiments were conducted in the Children's Hospital Gene Expression Core Laboratory supported by National Institutes of Health (NIH) Grant NS-40828. This work was also funded in part by NIH Grant AR-44345, Projects 1 and 3 of NS-40828, and generous support from the Lee and Penny Anderson Family Foundation, the Joshua Frase Foundation, and the Muscular Dystrophy Association of the USA. Louis M. Kunkel is an Investigator at the Howard Hughes Medical Institute.

REFERENCES

1. **Bakay M, Zhao P, Chen J, and Hoffman EP.** A web-accessible complete transcriptome of normal human and DMD muscle. *Neuromuscul Disord* 12, *Suppl* 1: S125–S141, 2002.
2. **Braunstein H.** Effect of postmortem interval on histochemical reactions of the myocardium. *Am J Clin Pathol* 49: 224–231, 1968.
3. **Breitkreutz BJ, Stark C, and Tyers M.** Osprey: a network visualization system. *Genome Biol* 4: R22, 2003.
4. **Calder PC and Geddes R.** Post mortem glycogenolysis is a combination of phosphorolysis and hydrolysis. *Int J Biochem* 22: 847–856, 1990.
5. **Castro-Alcaraz S, Miskolci V, Kalasapudi B, Davidson D, and Vancurova I.** NF-kappa B regulation in human neutrophils by nuclear I kappa B alpha: correlation to apoptosis. *J Immunol* 169: 3947–3953, 2002.
6. **Chandra J, Samali A, and Orrenius S.** Triggering and modulation of apoptosis by oxidative stress. *Free Radic Biol Med* 29: 323–333, 2000.
7. **Chang NS.** The non-ankyrin C terminus of Ikappa Balpha physically interacts with p53 in vivo and dissociates in response to apoptotic stress,

hypoxia, DNA damage, and transforming growth factor-beta 1-mediated growth suppression. *J Biol Chem* 277: 10323–10331, 2002.
8. **Chen YW, Zhao P, Borup R, and Hoffman EP.** Expression profiling in the muscular dystrophies: identification of novel aspects of molecular pathophysiology. *J Cell Biol* 151: 1321–1336, 2000.
9. **Clanton TL and Klawitter PF.** Adaptive responses of skeletal muscle to intermittent hypoxia: the known and the unknown. *J Appl Physiol* 90: 2476–2487, 2001.
10. **Clarkson PM and Sayers SP.** Etiology of exercise-induced muscle damage. *Can J Appl Physiol* 24: 234–248, 1999.
11. **Collan Y and Salmenpera M.** Electron microscopy of postmortem autolysis of rat muscle tissue. *Acta Neuropathol (Berl)* 35: 219–233, 1976.
12. **Coyle P, Philcox JC, Carey LC, and Rofe AM.** Metallothionein: the multipurpose protein. *Cell Mol Life Sci* 59: 627–647, 2002.
13. **Das DK, Maulik N, and Moraru II.** Gene expression in acute myocardial stress. Induction by hypoxia, ischemia, reperfusion, hyperthermia and oxidative stress. *J Mol Cell Cardiol* 27: 181–193, 1995.
14. **Dasika GK, Lin SC, Zhao S, Sung P, Tomkinson A, and Lee EY.** DNA damage-induced cell cycle checkpoints and DNA strand break repair in development and tumorigenesis. *Oncogene* 18: 7883–7899, 1999.
15. **Davies KJ.** Intracellular proteolytic systems may function as secondary antioxidant defenses: an hypothesis. *J Free Radic Biol Med* 2: 155–173, 1986.
16. **Deng Y, Pang A, and Wang JH.** Regulation of mammalian STE20-like kinase 2 (MST2) by protein phosphorylation/dephosphorylation and proteolysis. *J Biol Chem* 278: 11760–11767, 2003.
17. **Eguchi Y, Eguchi N, Oda H, Seiki K, Kijima Y, Matsu-ura Y, Urade Y, and Hayaishi O.** Expression of lipocalin-type prostaglandin D synthase (beta-trace) in human heart and its accumulation in the coronary circulation of angina patients. *Proc Natl Acad Sci USA* 94: 14689–14694, 1997.
18. **Eisen MB, Spellman PT, Brown PO, and Botstein D.** Cluster analysis and display of genome-wide expression patterns. *Proc Natl Acad Sci USA* 95: 14863–14868, 1998.
19. **Greenberg SA, Sanoudou D, Haslett JN, Kohane IS, Kunkel LM, Beggs AH, and Amato AA.** Molecular profiles of inflammatory myopathies. *Neurology* 59: 1170–1182, 2002.
20. **Haslett JN, Sanoudou D, Kho AT, Bennett RR, Greenberg SA, Kohane IS, Beggs AH, and Kunkel LM.** Gene expression comparison of biopsies from Duchenne muscular dystrophy (DMD) and normal skeletal muscle. *Proc Natl Acad Sci USA* 99: 15000–15005, 2002.
21. **Haslett JN, Sanoudou D, Kho AT, Han M, Bennett RR, Kohane IS, Beggs AH, and Kunkel LM.** Gene expression profiling of Duchenne muscular dystrophy skeletal muscle. *Neurogenetics* 4: 163–171, 2003.
22. **Huff-Lonergan E, Parrish FC Jr, and Robson RM.** Effects of postmortem aging time, animal age, and sex on degradation of titin and nebulin in bovine longissimus muscle. *J Anim Sci* 73: 1064–1073, 1995.
23. **Kallio PJ, Wilson WJ, O'Brien S, Makino Y, and Poellinger L.** Regulation of the hypoxia-inducible transcription factor 1alpha by the ubiquitin-proteasome pathway. *J Biol Chem* 274: 6519–6525, 1999.
24. **Klee CB, Crouch TH, and Richman PG.** Calmodulin. *Annu Rev Biochem* 49: 489–515, 1980.
25. **Lee JC and Peter ME.** Regulation of apoptosis by ubiquitination. *Immunol Rev* 193: 39–47, 2003.
26. **Leung CH, Lam W, Zhuang WJ, Wong NS, Yang MS, and Fong WF.** PKCdelta-dependent deubiquitination and stabilization of Gadd45 in A431 cells overexposed to EGF. *Biochem Biophys Res Commun* 285: 283–288, 2001.
27. **Mayer M and Neufeld B.** Post-mortem changes in skeletal muscle protease and creatine phosphokinase activity: a possible marker for determination of time of death. *Forensic Sci Int* 15: 197–203, 1980.
28. **Mikami H, Terazawa K, Takatori T, Tokudome S, Tsukamoto T, and Haga K.** Estimation of time of death by quantification of melatonin in corpses. *Int J Legal Med* 107: 42–51, 1994.
29. **Murphy BJ, Andrews GK, Bittel D, Discher DJ, McCue J, Green CJ, Yanovsky M, Giaccia A, Sutherland RM, Laderoute KR, and Webster KA.** Activation of metallothionein gene expression by hypoxia involves metal response elements and metal transcription factor-1. *Cancer Res* 59: 1315–1322, 1999.
30. **Porter JD, Khanna S, Kaminski HJ, Rao JS, Merriam AP, Richmonds CR, Leahy P, Li J, Guo W, and Andrade FH.** A chronic inflammatory response dominates the skeletal muscle molecular signature in dystrophin-deficient mdx mice. *Hum Mol Genet* 11: 263–272, 2002.
31. **Razeghi P, Faadiel Essop M, Huss JM, Abbasi S, Manga N, and Taegtmeyer H.** Hypoxia-induced switches of myosin heavy chain isogene expression in rat heart. *Biochem Biophys Res Commun* 303: 1024–1027, 2003.
32. **Rouger K, Le Cunff M, Steenman M, Potier MC, Gibelin N, Dechesne CA, and Leger JJ.** Global/temporal gene expression in diaphragm and hindlimb muscles of dystrophin-deficient (mdx) mice. *Am J Physiol Cell Physiol* 283: C773–C784, 2002. First published April 24, 2002; 10.1152/ajpcell.00112.2002.
33. **Sanoudou D, Haslett JN, Kho AT, Guo S, Gazda HT, Greenberg SA, Lidov HG, Kohane IS, Kunkel LM, and Beggs AH.** Expression profiling reveals altered satellite cell numbers and glycolytic enzyme transcription in nemaline myopathy muscle. *Proc Natl Acad Sci USA* 100: 4666–4671, 2003.
34. **Seoane J, Le HV, and Massague J.** Myc suppression of the p21(Cip1) Cdk inhibitor influences the outcome of the p53 response to DNA damage. *Nature* 419: 729–734, 2002.
35. **Stuart CA, Wen G, and Jiang J.** GLUT3 protein and mRNA in autopsy muscle specimens. *Metabolism* 48: 876–880, 1999.
36. **Takekawa M and Saito H.** A family of stress-inducible GADD45-like proteins mediate activation of the stress-responsive MTK1/MEKK4 MAPKKK. *Cell* 95: 521–530, 1998.
37. **Tkatchenko AV, Le Cam G, Leger JJ, and Dechesne CA.** Large-scale analysis of differential gene expression in the hindlimb muscles and diaphragm of mdx mouse. *Biochim Biophys Acta* 1500: 17–30, 2000.
38. **Tokunaga I, Takeichi S, Yamamoto A, Gotoda M, and Maeiwa M.** Comparison of postmortem autolysis in cardiac and skeletal muscle. *J Forensic Sci* 38: 1187–1193, 1993.
39. **Trump BF and Berezesky IK.** The reaction of cells to lethal injury. In: *When Cells Die*, edited by Lockshin RA and Zakeri Z. New York: Wiley, 1998, p. 57–96.
40. **Tseng BS, Zhao P, Pattison JS, Gordon SE, Granchelli JA, Madsen RW, Folk LC, Hoffman EP, and Booth FW.** Regenerated mdx mouse skeletal muscle shows differential mRNA expression. *J Appl Physiol* 93: 537–545, 2002. First published April 19, 2002; 10.1152/japplphysiol.00202.2002.
41. **Tusher VG, Tibshirani R, and Chu G.** Significance analysis of microarrays applied to the ionizing radiation response. *Proc Natl Acad Sci USA* 98: 5116–5121, 2001.
42. **Utz PJ and Anderson P.** Life and death decisions: regulation of apoptosis by proteolysis of signaling molecules. *Cell Death Differ* 7: 589–602, 2000.
43. **Vogt M, Puntschart A, Geiser J, Zuleger C, Billeter R, and Hoppeler H.** Molecular adaptations in human skeletal muscle to endurance training under simulated hypoxic conditions. *J Appl Physiol* 91: 173–182, 2001.
44. **Wang GL, Jiang BH, Rue EA, and Semenza GL.** Hypoxia-inducible factor 1 is a basic-helix-loop-helix-PAS heterodimer regulated by cellular O_2 tension. *Proc Natl Acad Sci USA* 92: 5510–5514, 1995.
45. **Wang KK, Villalobo A, and Roufogalis BD.** Calmodulin-binding proteins as calpain substrates. *Biochem J* 262: 693–706, 1989.
46. **Yan Z, Choi S, Liu X, Zhang M, Schageman JJ, Lee SY, Hart R, Lin L, Thurmond FA, and Williams RS.** Highly coordinated gene regulation in mouse skeletal muscle regeneration. *J Biol Chem* 278: 8826–8836, 2003.
47. **Yoshimura M, Nakamura S, Ito T, Nakayama M, Harada E, Mizuno Y, Sakamoto T, Yamamuro M, Saito Y, Nakao K, Yasue H, and Ogawa H.** Expression of aldosterone synthase gene in failing human heart: quantitative analysis using modified real-time polymerase chain reaction. *J Clin Endocrinol Metab* 87: 3936–3940, 2002.